

# CATALYTIC PROPERTIES OF THERMALLY DECOMPOSED 12-MOLYBDOPHOSPHORIC AND 10-MOLYBDO-2-VANADOPHOSPHORIC ACIDS

In Kyu SONG, Sang Heup MOON and Wha Young LEE\*

Department of Chemical Engineering, Seoul National University,  
Shinlim-dong San 56-1, Kwanak-ku, Seoul 151-742, Korea  
(Received 5 October 1990 • accepted 29 November 1990)

**Abstract**—Changes in the structural and surface properties of 12-molybdophosphoric (abbreviated as  $\text{PMo}_{12}$ ) and 10-molybdo-2-vanadophosphoric (abbreviated as  $\text{PMo}_{10}\text{V}_2$ ) acids as they are decomposed at high temperatures have been studied by IR, XRD, XPS, and TPD experiments.  $\text{PMo}_{12}$  simply decomposes into  $\text{MoO}_3$  by heat-treatment at 580°C, but  $\text{PMo}_{10}\text{V}_2$  yields a mixed oxide whose properties are different from those of either  $\text{MoO}_3$  or  $\text{V}_2\text{O}_5$ . After the thermal decomposition,  $\text{PMo}_{12}$  loses the initial acidic and redox properties almost completely but  $\text{PMo}_{10}\text{V}_2$  retains some extent of the redox capability that is larger than that of  $\text{MoO}_3$  and  $\text{V}_2\text{O}_5$ . The redox capability of the mixed oxide obtained by  $\text{PMo}_{10}\text{V}_2$  decomposition is correlated with its catalytic activity in oxidation processes.

## INTRODUCTION

Heteropoly compounds are acids and at the same time oxidizing agents [1-4]. Taking advantage of these properties, heteropoly compounds have been used as catalysts for various synthesis reactions [5-8]. However, a common weak point of the heteropoly compounds is that they are easily decomposed at elevated temperatures and therefore they experience severe deactivation under the reaction conditions of high temperature. In this study, 12-molybdophosphoric acid,  $\text{H}_2\text{PMo}_{12}\text{O}_{40}$ , and 10-molybdo-2-vanadophosphoric acid,  $\text{H}_2\text{PMo}_{10}\text{V}_2\text{O}_{40}$ , have been decomposed at different temperatures, and changes in their structural and surface properties have been investigated by XRD, IR, and XPS. In addition, the acidic and redox properties of the thermally decomposed compounds have been measured, and the results have been correlated with their catalytic activity in oxidation processes.

## EXPERIMENTAL

### 1. Catalyst preparation

$\text{PMo}_{12}$  and  $\text{PMo}_{10}\text{V}_2$  have been prepared following the procedures of Tsigdinos [9] and by the extraction

method [10]. The Keggin structure characteristic to the heteropoly acids has been confirmed by IR spectrum observation. For thermal decomposition, the catalyst samples have been put in a reactor and the reactor has been heated to and maintained at high temperatures in flowing  $\text{N}_2$ .

### 2. IR and TPD spectrum

For IR spectrum observation, the catalyst and KBr powder have been mixed and pressed into a thin self-supporting sample wafer. The IR spectra have been recorded with FT-IR spectrometer (Bomen DA 3.02) using KBr as a reference wafer.

Temperature-programmed desorption (TPD) of pre-adsorbed pyridine from the catalyst samples have been measured using a vacuum-tight flow reactor. After thermal treatments, the catalyst samples have been cooled to 60°C in the reactor, and pyridine has been injected into the reactor as pulses in  $\text{N}_2$  stream until no further adsorption of pyridine is observed. The reactor is then evacuated at 130°C for 1 hour so that physisorbed pyridine is removed from the sample. After cooling to room temperature, the reactor is heated again at 8°C/min up to 700°C as the amounts of desorbing pyridine in the out-flowing stream is monitored by flame ionization detector (FID).

### 3. Extents of reduction and reoxidation

The catalyst samples have been reduced in a simultaneous reactor/microbalance shown in Fig. 1 by flow-

\*To whom correspondence related to this paper should be made.

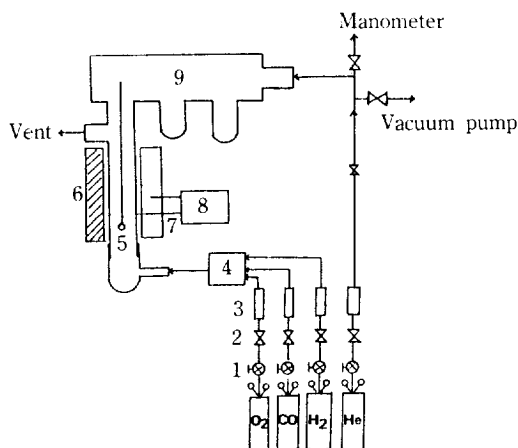


Fig. 1. Apparatus used for active lattice-oxygen measurement.

1. Pressure regulator
2. Needle valve
3. Rotameter
4. On-off valve
5. Sample tare
6. Electric furnace
7. Thermocouple
8. Temperature controller
9. Cahn 2000 electrobalance

ing  $H_2$  mixed with He ( $H_2/He=3/2$ , total flow rate = 200 ml/min) at  $300^\circ C$ , and the extent of reduction has been measured from the sample weight loss. The extent of reoxidation of the sample has also been measured in the same apparatus by flowing  $O_2$  in He stream ( $O_2/He=3/8$ , total flow rate = 110 ml/min) at  $300^\circ C$ .

#### 4. Reaction tests

Rates of CO oxidation on the catalysts have been measured in a differential micro-reactor unit. The reactor is a 1/4" stainless-steel tube with a thermocouple imbedded in the catalyst bed. The reactant stream contains 4.5% CO in air, and the product stream is analyzed by a gas chromatograph (GC) equipped with a thermal conductivity detector (TCD). Similar unit has been used for o-xylene oxidation on the catalysts. Differences are that in the latter case an extra micro-feeder is connected to the reactor for injection of the liquidus o-xylene and that the product stream is analyzed by GC with a flame ionization detector (FID). Details of the experimental procedure are given elsewhere [11].

## RESULTS AND DISCUSSION

### 1. Structural changes with thermal decomposition

#### 1-1. XRD study

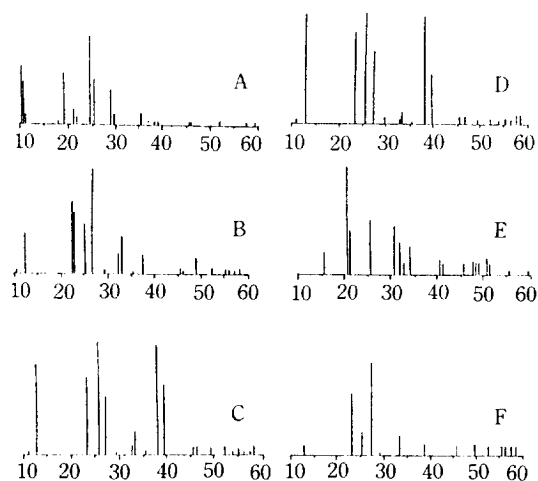


Fig. 2. XRD patterns of the heteropoly compounds after various thermal treatments.

- A.  $H_3PMO_{12}O_{40}$  calcined at  $280^\circ C$
- B.  $H_3PMO_{12}O_{40}$  calcined at  $430^\circ C$
- C.  $H_3PMO_{12}O_{40}$  calcined at  $700^\circ C$
- D.  $MoO_3$
- E.  $V_2O_5$
- F.  $H_3PMO_{10}V_2O_{40}$  calcined at  $580^\circ C$

Fig. 2 shows changes in the XRD patterns of  $PMO_{12}$  and  $PMO_{10}V_2$  as they are decomposed in an inert atmosphere at different temperatures. The characteristic XRD pattern of  $PMO_{12}$  changes gradually as the sample is treated at higher temperatures, and the pattern eventually becomes the same as that of  $MoO_3$  after treatment at  $580^\circ C$ . This agrees with the current understanding [11] that  $PMO_{12}$  is readily decomposed to  $MoO_3$  above  $430^\circ C$ .

Contrary to this,  $PMO_{10}V_2$  does not decompose into  $MoO_3$  and  $V_2O_5$  completely after treatment at  $580^\circ C$ . This is supported by the XRD pattern of the  $580^\circ C$ -decomposed  $PMO_{10}V_2$  is not the same as any of the patterns of  $MoO_3$  and  $V_2O_5$ . The thermally treated  $PMO_{10}V_2$  seems to yield a new mixed oxide whose structure is different from either of  $MoO_3$  or  $V_2O_5$ .

#### 1-2. IR study

The structural changes of  $PMO_{12}$  and  $PMO_{10}V_2$  with thermal treatments have been monitored by their IR spectrum change (Fig. 3). The  $280^\circ C$ -treated  $PMO_{12}$  shows four absorption bands in the range of  $700-1200\text{ cm}^{-1}$ , characteristic to the Keggin structure of heteropoly acids [12]. The spectrum, however, changes significantly when the sample is treated at  $430^\circ C$ , and eventually becomes identical to that of  $MoO_3$  after treatment at  $580^\circ C$ .

$PMO_{10}V_2$  treated at  $280^\circ C$  shows the characteristic 4-band structure of heteropoly acids. But, after treat-

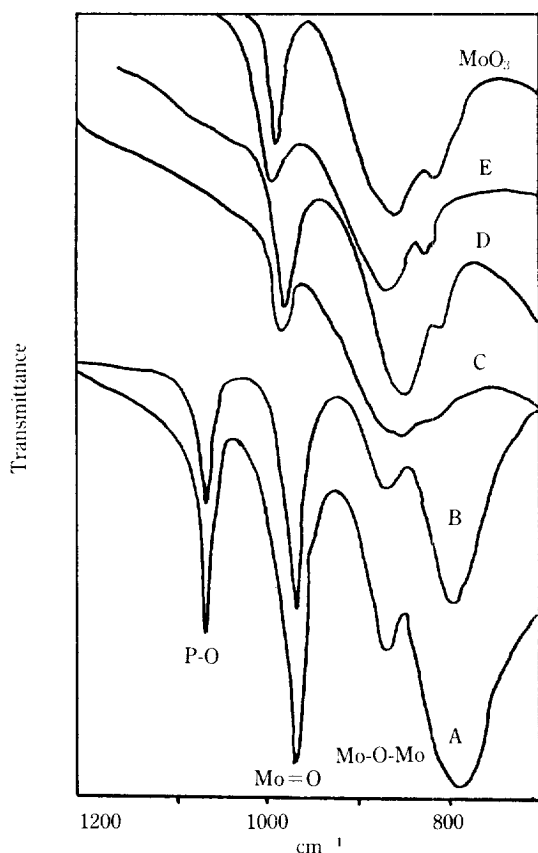


Fig. 3A. IR spectra of  $H_5PMo_{12}O_{40}$  after thermal treatment at given a temperature.

- |                   |          |
|-------------------|----------|
| A. No calcination | B. 280°C |
| C. 430°C          | D. 500°C |
| E. 700°C          |          |

ment at 580°C, the sample yields a new spectrum which is similar to neither of the spectrum from  $MoO_3$  or  $V_2O_5$ .

### 1-3. XPS study

Table I shows that the binding energy of Mo (3d) electron of the 580°C-decomposed  $PMo_{12}$  is the same as that of  $MoO_3$ . But, the 580°C-decomposed  $PMo_{10}V_2$  shows different binding energy of either Mo (3d) or V (2p) electron from that of  $MoO_3$  or  $V_2O_5$ . This suggests that the mixed oxide obtained by thermal decomposition of  $PMo_{10}V_2$  is a chemical compound within which Mo, V, and O atoms interact intimately with one another.

In conclusion, the above XRD, IR, and XPS results indicate that  $PMo_{10}V_2$  decomposed at 580°C yields a new mixed oxide whose property is different from that of a physical mixture of  $MoO_3$  and  $V_2O_5$ . On the

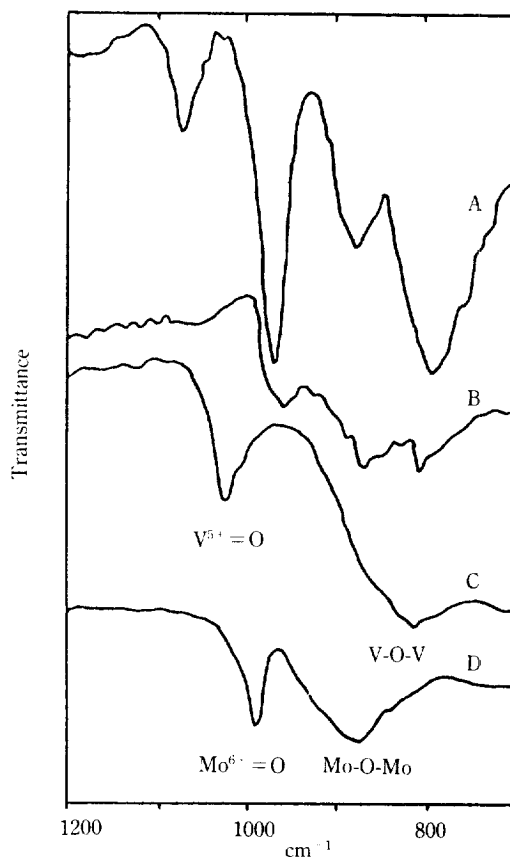


Fig. 3B. IR spectra of  $MoO_3$ ,  $V_2O_5$  and thermally decomposed  $H_5PMo_{10}V_2O_{40}$  acid.

- |                                             |
|---------------------------------------------|
| A. $H_5PMo_{10}V_2O_{40}$ calcined at 280°C |
| B. $H_5PMo_{10}V_2O_{40}$ calcined at 580°C |
| C. $V_2O_5$                                 |
| D. $MoO_3$                                  |

other hand,  $PMo_{12}$  decomposes at 580°C simply into  $MoO_3$ .

## 2. Acidic and redox properties of the thermally decomposed oxides

### 2-1. Acidic property

Fig. 4 shows the spectra of pyridine desorption from the thermally decomposed  $PMo_{12}$ . The sample treated at 280°C shows three TPD peaks at 180, 425 and 557°C, indicating that its surface has three major acidic sites. The peaks gradually lose their initial intensity as the sample is treated at higher temperatures. After treatment at 580°C, the sample shows no pyridine desorption peak, indicating that it becomes almost non-acidic. Similar changes in the pyridine TPD spectra are observed on the thermally decomposed  $PMo_{10}V_2$ , although in this case the  $PMo_{10}V_2$  sample shows only two TPD peaks above 300°C. Accordingly, the well-known trend

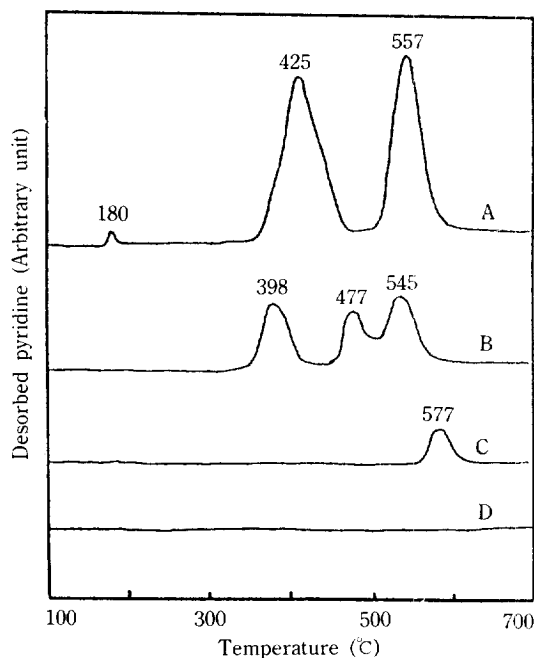


Fig. 4. TPD spectra of  $H_3PMo_{12}O_{40}$  after various thermal treatments.

- A.  $H_3PMo_{12}O_{40}$ , treated at 280°C
- B.  $H_3PMo_{12}O_{40}$ , treated at 430°C
- C.  $H_3PMo_{12}O_{40}$ , treated at 480°C
- D.  $H_3PMo_{12}O_{40}$ , treated at 580°C or 700°C  $MoO_3$

Table 1A. Binding energy of Mo (3d) in  $H_3PMo_{12}O_{40}$  after thermal treatment

Thermal treatment temperature (°C)	Binding energy (eV)	
Original crystal	240.7	237.5
280	240.6	237.5
430	240.5	237.4
500	241.0	238.0
580	241.4	238.2
	0.6	0.8
700	240.8	237.4
	0.7	0.8
$MoO_3$ (no treatment)	241.5	238.2

Table 1B. Binding energy(eV) of Mo(3d) and V(2p) in  $MoO_3$ ,  $V_2O_5$  and thermally decomposed  $H_5PMo_{10}V_2O_{40}$

Catalyst	Thermal treatment temperature (°C)	Mo (3d)		V (2p)		
$MoO_3$	no treatment	241.5	238.2			
		6.4	6.1			
$H_5PMo_{10}V_2O_{40}$	580°C	235.1	232.1	531.9	523.2	516.5
				3.2		
$V_2O_5$	no treatment			528.7	523.2	518.5

that heteropoly acids easily lose their Brønsted acidity by thermal decomposition has been confirmed by the TPD experiments.

#### 2-2. Redox property

Changes in the redox capability of the  $PMo_{12}$  and  $PMo_{10}V_2$  samples as they are decomposed at various temperatures have been measured by  $H_2$  reduction and reoxidation, and Fig. 5 shows the typical trend observed for  $Mo_{10}V_2$ .

The reason why the extent of reoxidation is smaller than that of  $H_2$ -reduction is because the sample partially loses the initial Keggin structure during the reduction process. As expected,  $PMo_{10}V_2$  loses significantly its initial redox capability by the thermal treatments. But, the sample still retains some extent of the initial redox capability even after treatment at 580°C, and the capability is significantly higher than that of  $MoO_3$  and  $V_2O_5$ . Accordingly, we have produced a new mixed oxide by thermal decomposition of  $PMo_{10}V_2$  at 580°C, which is stabler than the initial  $PMo_{10}V_2$  and has the redox capability larger than that of  $V_2O_5$  or  $MoO_3$ .

#### 2-3. Catalytic activity of the thermally decomposed oxides

Difference in the redox capability of  $PMo_{10}V_2$  and its thermally-decomposed sample is also observed in their catalytic activity for oxidation processes. Fig. 6 compares the rates of o-xylene oxidation on the  $PMo_{10}V_2$  catalysts obtained before or after the thermal decomposition. Since the oxidation process is highly exothermic, the rates are thermally accelerated when the heat of reaction accumulates in the reactor due to insufficient heat removal. Fig. 6 shows that the rate acceleration occurs at higher temperatures on the 580°C-decomposed  $PMo_{10}V_2$  than on the fresh  $PMo_{10}V_2$ , thus indicating that the former catalyst is less active than the latter. This agrees with the above result that  $PMo_{10}V_2$  has lost its initial redox capability by the thermal treatments.

We also have compared the activity in CO oxidation of the 580°C-decomposed  $PMo_{10}V_2$  with that of  $MoO_3$  and  $V_2O_5$ . Fig. 7 shows that the activity of the mixed oxide obtained by decomposition of  $PMo_{10}V_2$  at 580°C

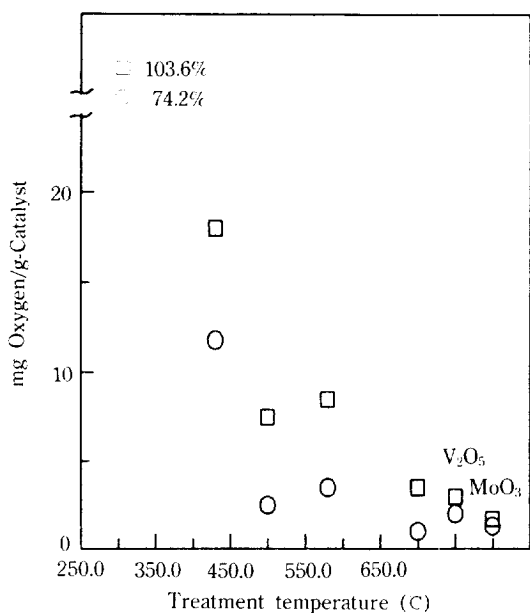


Fig. 5. Degree of reduction and reoxidation of  $H_5PMo_{10}V_2O_{40}$  at 300C after thermal treatment at a given temperature.

□ Degree of reduction, ○ Degree of reoxidation

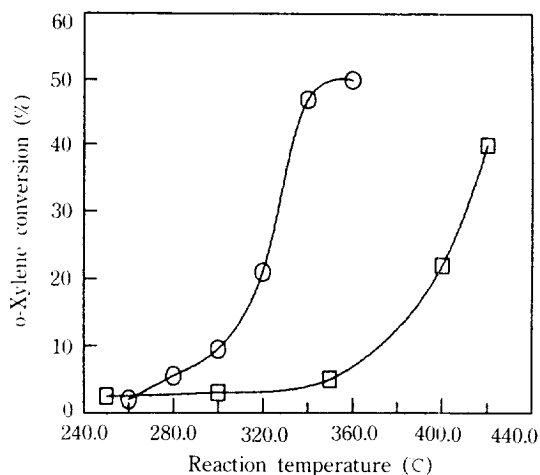


Fig. 6. Catalytic activity of  $H_5PMo_{10}V_2O_{40}$  before/after thermal decomposition in *o*-xylene oxidation.

○ Before thermal decomposition, □ After thermal decomposition at 580C

is higher than that of  $MoO_3$  or  $V_2O_5$ , again in agreement with the results of the redox capability observation.

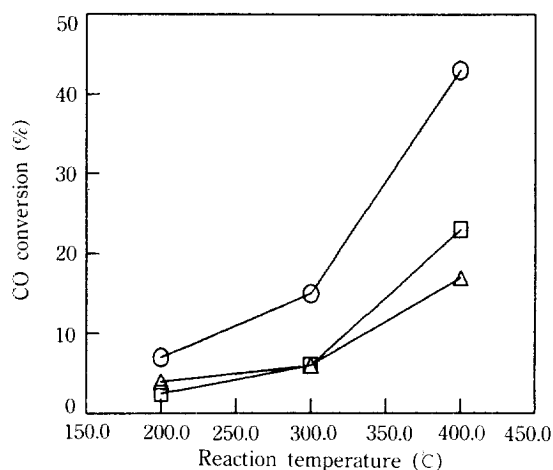


Fig. 7. Catalytic activity of 580C-decomposed  $H_5PMo_{10}V_2O_{40}$  and its constituent metal oxides in CO oxidation.

○ 580C-decompose  $H_5PMo_{10}V_2O_{40}$ , □  $V_2O_5$ , △  $MoO_3$

## CONCLUSIONS

The XRD, IR, and XPS results consistently show that, after thermal treatment at 580C,  $PMo_{12}$  decomposes into  $MoO_3$  but  $PMo_{10}V_2$  yields a new mixed oxide whose chemical properties are different from those of  $MoO_3$  or  $V_2O_5$ . After the thermal decomposition,  $PMo_{10}V_2$  loses the initial acidity almost completely as evidenced by the pyridine TPD experiments, but retains the redox capability to some extent, the extent being larger than that of  $MoO_3$  and  $V_2O_5$ . Accordingly, the mixed oxide obtained by decomposition of  $PMo_{10}V_2$  is stabler than the original  $PMo_{10}V_2$  and has larger redox capability than  $MoO_3$  or  $V_2O_5$ . The 580C-decomposed  $PMo_{10}V_2$  has a lower oxidation activity than the undecomposed  $PMo_{10}V_2$  but has a higher activity than  $MoO_3$  or  $V_2O_5$ , which is in agreement with the redox capability observation.

## ACKNOWLEDGEMENT

The authors appreciate the financial support by the Korea Science and Engineering Foundation for this work.

## REFERENCES

1. Tsigdinos, G. A.: *Topics Curr. Chem.*, **76**, 1 (1978); Sasaki, Y. and Matsumoto, K.: *Kagaku no Ryoiki*, **29**, 835 (1975).

2. Komata, T. and Mosono, M.: *Chemistry Letters*, 1177 (1983).
3. Yoshida, S., Niyama, H. and Echigoya, E.: *J. Phys. Chem.*, **86**, 3150 (1982).
4. Mizuno, M., Watanabe, T. and Misono, M.: *J. Phys. Chem.*, **89**, 80 (1985).
5. Onoue, Y., Mizutani, Y., Akiyama, S. and Izumi, Y.: *Chemtech.*, July, 432 (1978).
6. Misono, M., Sakata, K., Yoneda, Y. and Lee, W. H.: Proc. 7th Int. Con. Catal., 1047 (1980), Kodansha, Tokyo-Elsevier, Amsterdam (1981).
7. Akimoto, M., Shima, K., Ikeda, H. and Echigoya, E.: *J. Catal.*, **86**, 173 (1981).
8. Eguchi, K., Aso, I., Yamazoe, N. and Seiyama, T.: *Chemistry Letters*, 1345 (1979).
9. Tsigdinos, G. A.: *Ind. Eng. Chem. Res. Dev.*, **13**, 4 (1974).
10. Tsigdinos, G. A. and Hallada, C. J.: *Inorganic Chemistry*, **7**, 437 (1968).
11. Song, I.K.: M.S. Thesis, Seoul National Univ., Seoul, Korea (1989).
12. Furata, M., Sadata, K. and Misono, M.: *Chemistry Letters*, 31 (1979).